

# Electric field mathematical modelling at probe measurement in anisotropic semiconductor films

Filippov V.V.<sup>1,2</sup>, Mitsuk S.V.<sup>1</sup>, Lusyanin S.E.<sup>1</sup>

*Institute of Natural, Mathematical and Technical Sciences*

<sup>1</sup> *Lipetsk state pedagogical university of P. P. Semenov-Tyan-Shansky*

<sup>2</sup> *Southwest state university, Kursk*

Lipetsk, Russian Federation

wwfilippov@mail.ru, directorat-IEMiTN@yandex.ru, luzyanin\_se@mail.ru

**Abstract** – *The distribution of constant electric current potential in case of probe measurement on anisotropic semiconductors and fields has been studied. The expressions for potential distribution have been obtained. It enables to identify the area of the probe field of the scanning microscope in case an anisotropic film is under study. The results of the research demonstrate the correlation between the size and anisotropy of specific electroconductivity and the resistance change of probe spreading in limited films.*

**Keywords** – *anisotropic semiconductor, film, potential distribution, electroconductivity, spreading resistance, probe.*

## • Introduction

Semiconductor films of different structures are more and more widely used in production of micro- and nanoelectronics structures. The reduction of semiconductor thickness to submicronic causes inhomogeneities of various kinds in distribution of free charge carriers and anisotropy [1,2]. The scope of the observed phenomena, connected with charge transfer, is much wider in anisotropic than in isotropic semiconductors.

In special literature one can find the description of the change in charge carrier mobility in silicium and germanium in case of deformation, the change in effective masses and other factors leading to artificial anisotropy in film of nanometric thickness [1,3]. It is known that it is necessary to take into account the change of conductivity along different directions while studying electric fields in the film area, including the cases when they are studied by means of scanning probe microscopy [4,5].

One of the most verifiable ways of specific electroconductivity measurement is the method of spreading resistance reflection, which is available for a standard atomic-force microscope. The method works the following way: scanning is performed by the conducting probe AFM of the microscope in a contact mode and in this case the pressing force of the probe to the surface is kept constant.

The bias voltage is put to the probe and the resulting current through the sample, depending on the probe position, is registered. The second contact to the sample under the study is a plane of junction of the sample with the conductive backing. So, we simultaneously obtain the information about the surface relief pattern and the conductivity map.

The value of the measured current is proportional to local resistance of the sample under study is case the contact resistance and the given voltage remain unchanged.

It is contact resistance that introduces the basic error, that is why it is necessary to clean thoroughly the scanned plane of the film or the crystal. While measuring current-voltage characteristics the probe can settle above the surface rather long and, as a result, cause overheating of the sample and a change in resistance in this particular place. Not to expose the sample surface to such an influence it makes sense to use each session of scanning in a spreading resistance mode as a separate point for a current-voltage characteristic.

For practical research work experimenters and engineers must take into account a number of factors: the final sizes and the shapes of samples, the angle of crystallographic direction orientation to the sample boundaries, location and sizes of the current contacts and etc. These data determines the accuracy of the drawn conductivity map. The problem here lies mainly in a complicated character of electric potential distribution and current distribution in samples, characterized by anisotropy of electrical parameters. These issues are not fully described in special literature.

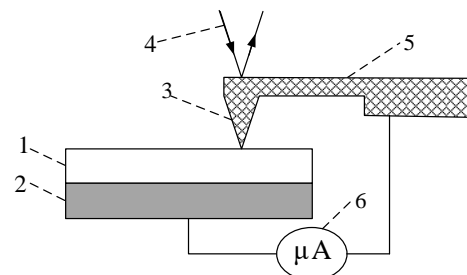


**Fig. 1.** Measurement Diagram in the mode reflecting spreading resistance

This graph in simplified form shows a probe pickup to make measurements in the mode of spreading resistance, where 1 – the sample under study, 2 – metal backing, 3 – probe, 4 – laser ray, 5 – cantilever, 6 – amperemeter.

So, the aim of this work is to analyze the anisotropy influence on potential distribution of the current probe in case of scanning a semiconductor film with a tensor conductivity. The main tasks are to obtain theoretical expressions for calculating electric field distribution and their further analysis. Another task is to study the influence of boundaries and electroconductivity of the sample on the value of the probe spreading resistance.

- Theoretical calculation of electric potential

Let us consider the distribution of the current probe potential to the anisotropic semiconductor film (fig. 2a).

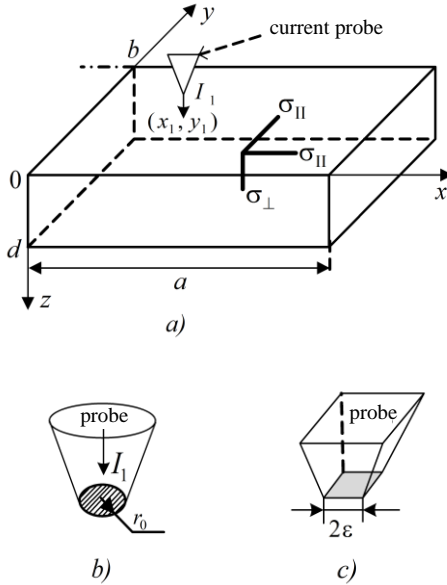


**Fig. 2.** a) The scheme of current probe location to the film under the study.  $I_1$  – probe current;  $(x_1, y_1)$  – coordinates of current probe center;  $a, b, d$  – geometrical sizes of the film; b) the form of the contact in case when the influence of boundaries is not taken into account; c) the form of contact in case when the influence of boundaries is taken into account.

It is convenient to represent the tensor of special electroconductivity in Cartesian coordinate system in the following way [11]:

$$\hat{\sigma} = \begin{pmatrix} \sigma_{\parallel} & 0 & 0 \\ 0 & \sigma_{\parallel} & 0 \\ 0 & 0 & \sigma_{\perp} \end{pmatrix}, \quad (1)$$

where  $\sigma_{\perp}$  – value of special electroconductivity along  $z$ -axis;  $\sigma_{\parallel}$  – special conductivity along  $x$ -axis and  $y$ -axis. Anisotropy of this kind can be caused by the crystal structure or by the defor-

mation influence [4-7], and also appears in quantum-dimensional films [1,2].

The equation for the electrical potential can be presented in the following form [11,12]:

$$\sigma_{\parallel} \frac{\partial^2 \varphi}{\partial x^2} + \sigma_{\parallel} \frac{\partial^2 \varphi}{\partial y^2} + \sigma_{\perp} \frac{\partial^2 \varphi}{\partial z^2} = 0. \quad (2)$$

By replacing in (2) a variable we will get Laplace equation:

$$\frac{\partial^2 \varphi}{\partial x^2} + \frac{\partial^2 \varphi}{\partial y^2} + \frac{\partial^2 \varphi}{\partial \xi^2} = 0, \quad (3)$$

$$\xi = \gamma z, \quad \gamma = \sqrt{\sigma_{\parallel} / \sigma_{\perp}}. \quad (4)$$

In case of an unlimited film it is convenient to use the cylindrical coordinate system in which the equation (3), according to [11,12] will acquire the form:

$$\frac{\partial^2 \varphi}{\partial r^2} + \frac{1}{r} \frac{\partial \varphi}{\partial r} + \frac{\partial^2 \varphi}{\partial \xi^2} = 0. \quad (5)$$

We fix the beginning of the cylindrical coordinate system in the center of the current probe. The boundary conditions for the potential come from the condition that the normal constituent of current density is equal to zero on the whole surface of the sample except the points under the current electrode point with the radius  $r_0$  (fig. 2b); we consider the potential of the low plane to be equal to zero:

$$\varphi|_{r \rightarrow \infty} = 0, \quad \varphi|_{\xi = \gamma d} = 0; \quad \frac{\partial \varphi}{\partial \xi} \Big|_{\xi=0} = \begin{cases} 0, & r > r_0; \\ -\frac{I_1}{\gamma \sigma_{\perp} \pi r_0^2}, & r \leq r_0. \end{cases} \quad (6)$$

Laplace equation with boundary conditions (6) can be represented in the form of Fourier-Bessel integral [12,13] and has a following solution:

$$\varphi(r, \xi) = \int_0^{\infty} \Phi(t, \xi) J_0(t \cdot r) t dt, \quad (7)$$

where coefficient  $\Phi(t, \xi)$  are determined by the equality:

$$\Phi(t, \xi) = \int_0^{\infty} \varphi(r, \xi) J_0(t \cdot r) r dr. \quad (8)$$

If we place the expression for the potential (7) in the equation (5) and multiply it by  $J_0(t \cdot r) r dr$ , integrate by  $r$  from 0 to  $\infty$  and consider the property of orthogonality of Bessel function [12,13], then for  $\Phi(t, \xi)$  we will have the equation:

$$\frac{d^2 \Phi}{d\xi^2} - t^2 \cdot \Phi = 0. \quad (9)$$

Consequently,

$$\Phi(t, \xi) = (A \cdot \text{sh}(t \cdot \xi) + B \cdot \text{ch}(t \cdot \xi)), \quad (10)$$

where consonants A and B are determined by the boundary conditions (6).

As a result the expression for the potential can

be represented in the form of:

$$\varphi(r, \xi) = -\frac{I_1}{\pi\gamma\sigma_{\perp}r_0} \int_0^{\infty} \frac{\text{sh}(t(\xi - \gamma d))}{t \cdot \text{ch}(t \cdot \gamma d)} J_0(t \cdot r) J_1(t \cdot r_0) dt. \quad (11)$$

Returning to the standard cylindrical coordinates we get:

$$\varphi(r, z) = -\frac{I_1}{\pi\gamma\sigma_{\perp}r_0} \int_0^{\infty} \frac{\text{sh}(t \cdot \gamma(z-d))}{t \cdot \text{ch}(t \cdot \gamma \cdot d)} J_0(t \cdot r) J_1(t \cdot r_0) dt. \quad (12)$$

After calculating the average value of the potential by the circle contact area we can find spreading resistance:

$$R_0 = \frac{2}{\pi\sigma_{\perp}\gamma r_0^2} \int_0^{\infty} \frac{\text{sh}(t \cdot \gamma \cdot d)}{t^2 \cdot \text{ch}(t \cdot \gamma \cdot d)} (J_1(t \cdot r_0))^2 dt. \quad (13)$$

In accordance with the obtained expression (13), the values, characterizing the current spreading in the film, are the area of the contact surface [13-16], the film thickness and anisotropy parameters.

To take into account the film boundaries let us consider potential distribution of the current probe to a rectangular anisotropic film (fig. 2a), let us represent the point of the probe as a square with the side  $2\varepsilon$  (fig. 2c). This particular shape of the contact area (unlike round) enables us to obtain an analytical solution for the potential in a rectangular sample. The contact surface shape of the current probe 3 (fig. 2) is difficult to control. The main parameter, determining spreading resistance for small probes (point probes), is the contact surface area but not its shape.

Boundary conditions for the potential in this case are presented in the following form:

$$\begin{aligned} \sigma_{\parallel} \frac{\partial \varphi}{\partial x} \Big|_{x=0,a} &= \sigma_{\parallel} \frac{\partial \varphi}{\partial y} \Big|_{y=0,b} = 0, \quad \varphi|_{z=d} = 0, \\ \sigma_{\perp} \frac{\partial \varphi}{\partial z} \Big|_{z=0} &= \begin{cases} -\frac{I_1}{4\varepsilon^2}, & x_1 - \varepsilon \leq x \leq x_1 + \varepsilon; \\ & y_1 - \varepsilon \leq y \leq y_1 + \varepsilon; \\ 0, & \text{in the rest of the area.} \end{cases} \end{aligned} \quad (14)$$

Here  $x_1$  and  $y_1$  – are coordinates of the movable probe, the planes of contact areas are parallel to the sample planes (fig. 2).

It seems convenient to represent the solution of the boundary problem (2), (14) for potential distribution in double Fourier series [17]:

$$\varphi(x, y, z) = \frac{I_1}{ab\sigma_{\perp}} [d - z] - \frac{4I_1}{ab\sigma_{\perp}} \sum_{n,k=0}^{\infty} \Theta_{nk} \frac{\text{sh}(\eta_{nk}(z-d))}{\eta_{nk} \text{ch}(\eta_{nk} d)} \frac{\sin(\alpha_n \varepsilon)}{\alpha_n \varepsilon} \frac{\sin(\beta_k \varepsilon)}{\beta_k \varepsilon} \cdot \cos(\alpha_n x_1) \cos(\beta_k y_1) \cos(\alpha_n x) \cos(\beta_k y) \quad (15)$$

$$\alpha_n = \frac{\pi n}{a}, \quad \beta_k = \frac{\pi k}{b}, \quad \eta_{nk} = \sqrt{\frac{\sigma_{\parallel}}{\sigma_{\perp}} (\alpha_n^2 + \beta_k^2)}$$

$$\Theta_{nk} = \begin{cases} 1, & n \neq 0 \wedge k \neq 0; \\ 1/2, & n = 0 \wedge k \neq 0 \vee n \neq 0 \wedge k = 0; \\ 0, & n = k = 0. \end{cases} \quad (16)$$

Then we find the value of spreading resistance of the limited anisotropic field:

$$R = \frac{d}{ab\sigma_{\perp}} + \frac{4}{d} \cdot \frac{d}{ab\sigma_{\perp}} \sum_{n,k=0}^{\infty} \Theta_{nk} \frac{\text{sh}(\eta_{nk} d)}{\eta_{nk} \text{ch}(\eta_{nk} d)} \times \left( \frac{\sin(\alpha_n \varepsilon)}{\alpha_n \varepsilon} \frac{\sin(\beta_k \varepsilon)}{\beta_k \varepsilon} \right)^2 \cdot \cos^2(\alpha_n x_1) \cos^2(\beta_k y_1) \quad (17)$$

In case of the point contacts ( $2\varepsilon \ll d, a, b$ ), in the expressions mentioned above (15), (17) we get the simplification:

$$\left( \frac{\sin(\alpha_n \varepsilon)}{\alpha_n \varepsilon} \frac{\sin(\beta_k \varepsilon)}{\beta_k \varepsilon} \right) \equiv 1. \quad (18)$$

One of principle conditions of applicability of the potential expressions (8), (15) is the presence of a smooth boundary on the plane, separating the contact and the metal surface. The influence of quantum and charge effects is not taken into account [1, 2, 11], which are especially noticeable at low temperatures.

It is known that in thin films at low temperatures ( $T \approx 0-10$  K) it is possible to observe the effect of electroconductivity quantization and ballistic transport of electrons and tunnel effects. The classical electrodynamic model can not describe such phenomena.

Nonhomogeneous distribution of doping material in the sample under study at simultaneous exposure to electric field and uneven heating can lead to appearance of areas of bulk charge, which change within time. That is the reason why the described theory of potential measurement and spreading resistance can not be applied to structures with bulk charge, which are exposed to uneven heating.

- Modelling of electrical fields of current probe

Let us model an electrical field at the section of a semiconductor film on the plane  $y = b/2$  with the side length  $a = b = 10d$ ,  $2\varepsilon = d$ , the contact is placed at the center of the film surface (fig. 3). The models of potential and current distribution are built on the basis of the expression (15) where  $x_1 = a/2$ ,  $y_1 = b/2$ . In figure 2 the total number of equipotentials on the sample section equals 20, the number of the current lines equals 10. Cadmium and zink diarsenide have anisotropy parameters close to those mentioned in fig. 3 (natural anisotropy). If semiconductors are deformed, special conductivity anisotropy can be observed (for silicon –  $\sigma_1/\sigma_2 = 1 \div 5$ ) [3, 4]).

From the built models of the potential distribution and the distribution of the current lines (fig. 3) it is clear that the increase of  $\sigma_{\perp}/\sigma_{\parallel}$  – anisotropy parameter leads to a considerable concentration of equipotentials and current lines in the area

under the contact, and correspondingly the reduction of  $\sigma_{\perp}/\sigma_{\parallel}$  – parameter leads to field spreading in the volume of the film.

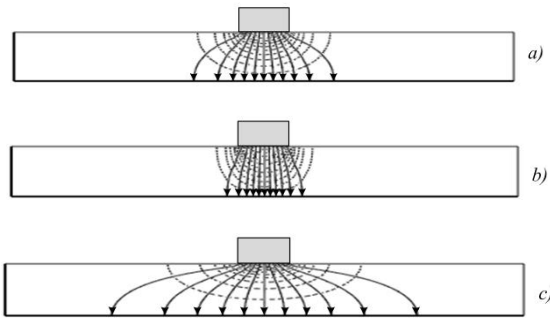


**Fig. 3.** Model of distribution of electric potential (dotted line) and current (full line) in anisotropic film; a)  $\sigma_{\parallel} = \sigma_{\perp}$ ; b)  $\sigma_{\parallel} = \sigma_{\perp}/5$ ; c)  $\sigma_{\parallel} = 5\sigma_{\perp}$ .

Let us draw the correlation between the film resistance, obtained according to (17), and the contact size (fig. 4). To analyze the influence of the boundaries we have calculated the ratio of resistance, which is calculated by the formula (17) to resistance of the limitless film (13) for the same contact surface area ( $4\varepsilon^2 = \pi r_0^2$ ).

In the case under study the semiconductor film has a shape of a square with the parameters  $a = b$ ,  $d = a/10$ . The probe with the contact width  $2\varepsilon = d$  is placed in the center of the film surface ( $x_1 = a/2$ ,  $y_1 = b/2$ ,  $z = 0$ ) (fig. 4).

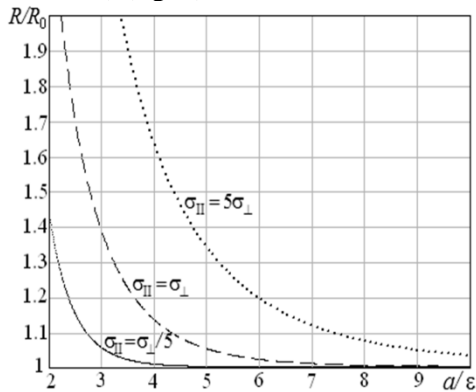


**Fig. 4.** The dependence of specific resistance from square size film ( $a = b$ ,  $d = a/10$ ) with parameters of electroconductivity  $\sigma_{\parallel} = \sigma_{\perp}/5$ ,  $\sigma_{\parallel} = \sigma_{\perp}$ ,  $\sigma_{\parallel} = 5\sigma_{\perp}$ .

It is noticeable (fig. 4) that the value of the anisotropy parameter  $\sigma_{\perp}/\sigma_{\parallel}$  has a strong influence on the value of spreading resistance. The influence of anisotropy and the sample boundaries is the most visible with the probe contact size  $2\varepsilon < a/20$ .

- Experimental testing

The experimental testing of the obtain distributions was carried out on anisotropic crystals cadmium diarsenide ( $\text{CdAs}_2$ ) and zink diarsenide ( $\text{ZnAs}_2$ ), which parameters are presented in the

following work [16]. Tungsten contact-logging probes were used in each case as current electrodes. In each case the potential value was identified with the help of a movable metal probe relating to the electrode which was grounded.

The constant current 0.05 A was passed through the sample from a stabilized supply source, the potential difference was measured with the help of a high resistance voltmeter. The error of measurement equipment was not more than 5%. The voltage was measured twice with different polarity of current. Figure 5 represents its average value. After the experimental potential value was obtained the diagrams of the corresponding theoretical dependences  $\varphi(x, y)$  were drawn, with the same current intensity through the sample. Figure 5 represents an example of correlation of the theoretical curve, drawn according to the potential distribution (15) with the experimental values for cadmium diarsenide ( $\sigma_{\perp} = 8.76 \text{ Om}^{-1} \cdot \text{m}^{-1}$ ,  $\sigma_{\parallel} = 40.96 \text{ Om}^{-1} \cdot \text{m}^{-1}$ ,  $a = 8.65 \text{ mm}$ ,  $b = 10.15 \text{ mm}$ ,  $d = 2.65 \text{ mm}$ ,  $2\varepsilon = 0.62 \text{ mm}$ ,  $x_1 = a/2$ ,  $y_1 = b/2$ ). The potential was measured on the crystal surface in the contact plane on the line  $y = b/2$ . Figure 6 represents the diagram of deviation of the experimental value from theoretical value  $\delta^2(x) = [(\varphi(\text{experimental}) - \varphi(\text{theoret.})) / \varphi(\text{theoret.})]^2$ .

The maximum deviations from theoretical values can be explained by non-homogeneities on the crystal surface. The calculated F-ratio test for matching theoretical and experimental points has the value of  $F = 0.092$  with critical for such amount of measurements value  $F_{\text{crit}} = 2.6$ . The obtained ratio of experimental and theoretical correlation is  $R_{\text{kor}} = 0.95$ . So, we obtained a good matching of theoretical data and theoretical potential distribution of the electric field within the measurement accuracy.

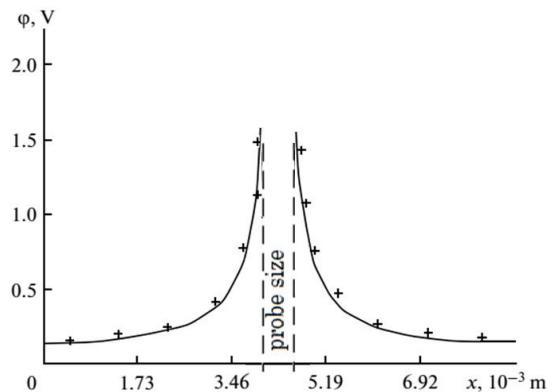


**Fig. 5.** Comparison of experimental data (+) and theoretical dependence (full line) of potential distribution on the line of the contact in semiconductor sample.

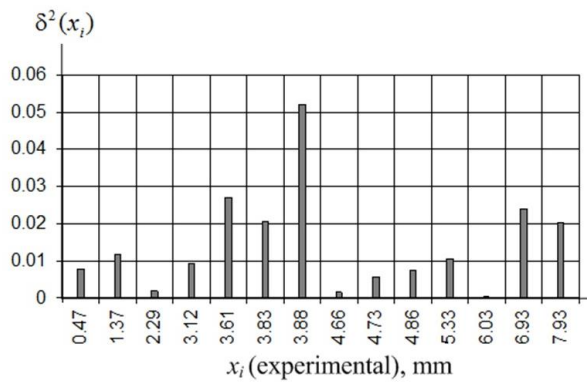


Fig. 6. Error diagram.

### • Conclusion

The research demonstrates that at probe measurement of electrophysical parameters of films with sub-micronic thickness the potential distribution depends considerably on anisotropy, the value of anisotropy parameter  $\sigma_{\perp}/\sigma_{\parallel}$  has a great influence on the resistance value of current probe spreading.

### References

- [1] Heikkila T. The Physics of Nanoelectronics. Oxford University, 2013
- [2] Dragoman M, Dragoman D. 2D Nanoelectronics, NanoScience and Technology. Springer International Publishing AG, 2017
- [3] Dragunov V P, Neizvestnyj I G and Gridchin V A. Osnovy nanoehlektroniki. Moscow: Logos, 2006
- [4] Schulze A, Loo R, Ryan P, et al. Observation and understanding of anisotropic strain relaxation in selectively grown SiGe fin structures. Nanotechnology, 2017, 28(14): 145703
- [5] Morrison C, Myronov M. Electronic transport anisotropy of 2D carriers in biaxial compressive strained germanium. Applied Physics Letters, 2017, 111 (19): 192103
- [6] Filippov V V, Vlasov A N, Bormontov E N. Modelling of electronic properties of strained silicon on a germanium substrate. Russian Physics Journal, 2014, 57(1): 55
- [7] Hassan A, Morris R, Mironov O, et al. Anisotropy in the hole mobility measured along the [110] and [101] orientations in a strained Ge quantum well. Applied Physics Letters, 2014, 104 (13):132108
- [8] Voigtlander B. Scanning Probe Microscopy. Atomic Force Microscopy and Scanning Tunneling Microscopy. Springer, Berlin, Heidelberg, 2015
- [9] Chen C J. Introduction to Scanning Tunneling Microscopy. Oxford University Press, 2015
- [10] Kalinin S, Gruverman A. Scanning Probe Microscopy. Electrical and Electromechanical Phenomena at the Nanoscale. Springer, New York, 2007
- [11] Nye J F. Physical properties of crystals their representation by tensors and matrices (Lecturer in Physics in the University of Bristol). Oxford at the Clarendon Press, 1957
- [12] Jackson J D. Classical Electrodynamics. John Wiley&Sons, Inc., 1962
- [13] Polyakov N N, Kon'kov V L. Spreading resistance of a flat circular contact. Soviet Physics Journal, 1970, 13 (9):1203
- [14] Schroder D K. Semiconductor Material and Device Characterization. John Wiley & Sons, Inc, 2006
- [15] Runyan W R, Shaffner T J. Semiconductor Measurements and Instrumentation. McGraw Hill Professional, 1998
- [16] Filippov V V. A technique for determining the electric conductivity and mobility of charge carriers in lamellar semiconductor materials. Instruments and Experimental Techniques, 2007, 50(4): 557-560
- [17] Filippov V V, Zavorotniy A A. Solution of Neumann boundary value problem for electrical field in anisotropic region at Hall measurements. Advanced Studies in Theoretical Physics, 2014, 8(25): 1135-1143